



Recognition of Mg^{2+} and Zn^{2+} based on a naphthalene-based fluorescent probe by regulating solvents



Jing-can Qin, Zheng-yin Yang*, Guan-qun Wang

College of Chemistry and Chemical Engineering, State Key Laboratory of Applied Organic Chemistry, Lanzhou University, Lanzhou 730000, PR China

ARTICLE INFO

Article history:

Received 14 May 2015

Received in revised form 25 June 2015

Accepted 26 June 2015

Available online 2 July 2015

Keywords:

Fluorescence probe

Naphthalene

Mg^{2+}/Zn^{2+}

Photo-induced electron transfer process

ABSTRACT

In this study, a naphthalene schiff-base which serves as a dual analyte chemosensor and quantifies Mg^{2+} and Zn^{2+} has been synthesized. The sensor shows “off–on” fluorescent response toward Mg^{2+} in acetonitrile while the detection of the sensor could be switched for Zn^{2+} by regulating solvents from acetonitrile to a mixture of ethanol–water (v/v, 4:1). Both of the sensing mechanisms are attributed to the formation of 1:1 ligand–metal complexes which inhibit photo-induced electron transfer (PET) process. More importantly, the reversibility of the recognition processes of HL is performed by adding a bonding agent Na_2EDTA .

© 2015 Elsevier B.V. All rights reserved.

1. Introduction

Magnesium is the eighth most abundant element on earth crust and has participated in many biological processes at the cellular level. For example, as an important trace element, Mg^{2+} has been involved in proliferation of cells, stabilization of DNA conformation, bone remodeling and skeletal development [1–5]. Selective detection of Mg^{2+} in the presence of other biologically relevant Ca^{2+} , Na^+ and K^+ or transition-metal ions is, therefore, of particular importance. However, the concentration of Mg^{2+} has still been poorly monitored because of the scarcity of efficient chemical tools.

Zinc, the second most abundant transition metal ion, is widely dispersed and used in our life, including in food additives, in medicines, and in the production of light alloys, etc. [6–7]. More importantly, as an essential element for human being, it plays very important role in series of physiological and pathological processes such as gene expression, regulation of metalloenzymes, neural signal transmission, cell apoptosis, DNA binding or recognition and so on [8–12]. Thus, a quantity of Zn^{2+} is beneficial for the people's health. But on the other hand, overloading condition, it exhibits toxicity in that it causes some overt toxicity symptoms and neurodegenerative disorders [13–16].

In order to protect the human health, it is crucial to develop several effective tools to detection of the concentration levels of Zn^{2+} and Mg^{2+} . In recent years, there are several methods which

are available for detection of Mg^{2+} and Zn^{2+} . However, they are generally expensive and time-consuming as well as inadequate for on-line monitoring [17–19]. Fluorescent chemosensor with high selectivity, sensitivity and real-time detection has been developed a convenient tool to detection of metal ions in analytical fields, especially multi-ion responsive molecular sensor which sense Mg^{2+} and Zn^{2+} simultaneously [20–23].

For these reasons, we have synthesized a schiff-base (HL) which was prepared by rhodamine and naphthalene moieties (Scheme 1). The receptor shows “off–on” fluorescent response toward Mg^{2+} in acetonitrile. On the other hand, the sensor could selectively response to Zn^{2+} in mixture of ethanol–water (v/v, 4:1). In addition, other relevant metal ions including Li^+ , Na^+ , K^+ , Ca^{2+} , Mg^{2+} , Cu^{2+} , Co^{2+} , Mn^{2+} , Ni^{2+} , Ba^{2+} , Fe^{2+} , Cd^{2+} , Hg^{2+} , Pb^{2+} , Fe^{3+} , Cr^{3+} , and Al^{3+} have no significant effect on the fluorescence both in acetonitrile or ethanol–water solvent.

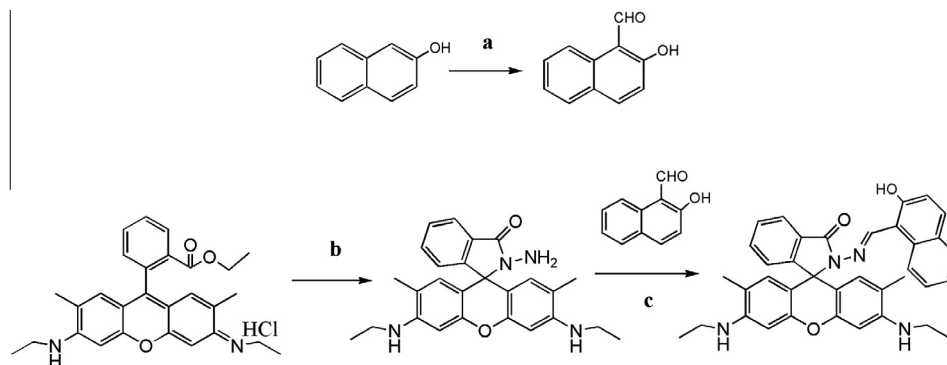
2. Experimental

2.1. Materials and instrumentation

Unless mentioned otherwise, all chemicals for synthesis were purchased from commercial suppliers and used without further purification. 1H NMR spectra were measured on the JNM-ECS 400 MHz instruments using TMS as an internal standard. ESI-MS were determined on a Bruker esquire 6000 spectrometer. UV–Vis absorption spectra were determined on a Shimadzu UV-240 spectrophotometer. Fluorescence spectra were recorded on a Hitachi RF-4500 spectrophotometer equipped with quartz cuvettes of

* Corresponding author. Tel.: +86 931 8913515; fax: +86 931 8912582.

E-mail address: yangzy@lzu.edu.cn (Z.-y. Yang).



Scheme 1. Reagents and conditions: (a) HMTA, glacial acetic acid, reflux, 6 h; (b) EtOH, N₂H₄·H₂O, reflux, 20 h; (c) EtOH, reflux, 12 h.

1 cm path length. The melting point was determined on a Beijing XT4-100x microscopic melting point apparatus.

Stock solutions of various cations (5 mM) were prepared using nitrate salts. A stock solution of HL (5 mM) was prepared, and then the stock solution was diluted 100 times.

2.2. Synthesis of the sensor (HL)

2-Hydroxy-1-naphthaldehyde (Fig. S1) and rhodamine 6G hydrazide (Fig. S2) were synthesized according to the method reported [24–25]. The synthetic route of the sensor was shown in Scheme 1. An ethanol solution of rhodamine 6G hydrazide (0.43 g, 1 mmol) was added to another ethanol containing 2-hydroxy-1-naphthaldehyde (1 mmol, 0.172 g), and then the mixture was stirred and refluxed for 12 h. After that, the final product was allowed to filtered, washed 3 times with 10 mL hot ethanol and dried under reduced pressure, the reaction afforded yellow solid, Yield: 65%. ¹H NMR (400 MHz; DMSO-d₆) (Fig. S3) δ (ppm) = 12.24 (s, H₁), 9.78 (s, H₁₀), 8.03 (m, H₁₁), 7.79 (d, H₃, J = 8.6 Hz), 7.65 (m, H₄, H₇), 7.53 (m, H₆, H₁₃), 7.43 (m, H₁₂), 7.33 (m, H₁₄), 7.11 (m, H₂, H₅), 6.46 (s, H₈, H₁₅), 6.35 (s, H₂₀, H₂₁), 3.48 (s, H₁₇, H₂₂), 3.15–3.21 (q, 2H₁₈, 2H₂₃, J = 7.1 Hz), 1.82 (s, 3H₉, 3H₁₆), 1.16 (t, 3H₁₉, 3H₂₄, J = 7.1 Hz). ESI-MS (Fig. S4): [M+1]⁺: 583.25. IR (KBr, cm⁻¹) (Fig. S5): 3429.13, 1683.75, 1620.79. Elemental Anal. C₃₇H₃₄N₄O₃: Calc. C, 76.27; H, 5.88; N, 9.62. Found: C, 76.13; H, 5.91; N, 9.70.

3. Results and discussion

3.1. General information

The binding constant values were determined from the emission intensity data following the modified Benesi–Hildebrand equation [26–27].

$$\frac{1}{F - F_{\min}} = \frac{1}{K(F_{\max} - F_{\min})[M^{n+}]} + \frac{1}{F_{\max} - F_{\min}}$$

where F_{\min} , F , and F_{\max} were the emission intensities of the organic moiety considered in the absence of metal ion, at an intermediate metal ion concentration, and at a concentration of complete interaction, respectively, and where K was the binding constant concentration.

The detection limits were calculated with the following equation: detection limit $3\sigma/\lambda$, based on the fluorescence titration. Where σ was the standard deviation of blank measurements, and λ was the slope between intensity versus sample concentration [28].

3.2. UV–Vis analysis

The binding ability of L-M (Mg²⁺, Zn²⁺) was initially evaluated by the UV–Vis analysis upon addition of different amounts of metal ions in acetonitrile and in ethanol–water (v/v, 4:1), respectively. Firstly, the interaction of HL and Mg²⁺ was investigated as a function of the concentration of Mg²⁺. As shown in Fig. 1, the spectrum of the free HL showed a maximum absorption band at 375 nm, which can be assigned to $\pi \rightarrow \pi^*$ transition of naphthalene group [29–32]. With the increasing concentration of Mg²⁺, the absorption band at 375 nm gradually decreased and a new absorption band appeared at 439 nm with increasing intensity. Moreover, a clear isosbestic point at 400 nm was observed, which clearly indicated the presence of new complex in equilibrium with the receptor. When the UV–Vis analysis was carried out in aqueous media, the metal ion was changed from Mg²⁺ to Zn²⁺, as shown in Fig. 2, the trend of change of the latter was similar to the former, the only differences was the extent of variation of the absorption at 439 nm.

In addition, we could observed that the absorbance band from 500 nm to 550 nm not appeared, which indicated the rhodamine core was in the ring closed isomeric form both in the presence of Mg²⁺ and Zn²⁺ [33–34]. It meant that the interaction of HL with Mg²⁺/Zn²⁺ could not trigger the ring-opened reaction of the rhodamine spirolactam. Therefore, the reasons for all these changes

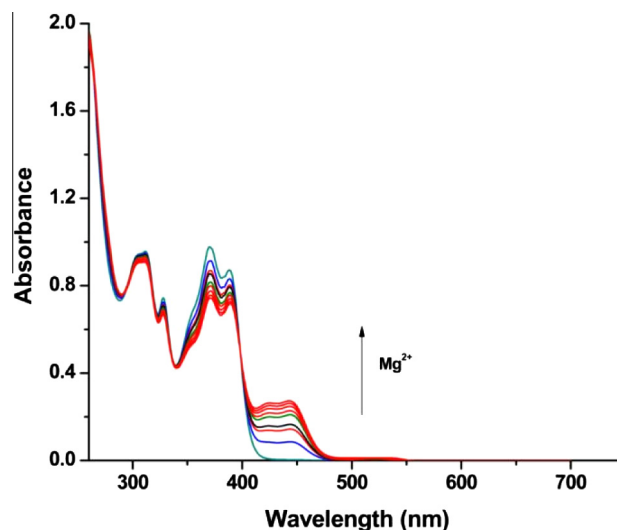


Fig. 1. Changes in the absorption spectra of HL (20 μM) in acetonitrile at room temperature as a function of added Mg²⁺ (0–1.0 equiv.).

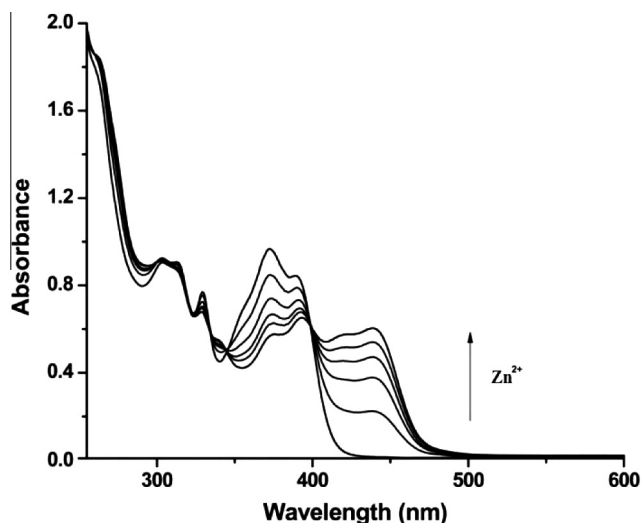


Fig. 2. Changes in the absorption spectra of HL (50 μM) in ethanol–water (v/v, 4:1) at room temperature as a function of added Zn^{2+} (0–1.0 equiv.).

should be ascribed to the chelation of the naphthalene moieties with $\text{Mg}^{2+}/\text{Zn}^{2+}$ rather than the ring-opening of the rhodamine spirolactam.

3.3. Selectivity studies and effects of metal ions

The selectivity of HL for Mg^{2+} was investigated in acetonitrile. As shown in Fig. 3. The free receptor showed weak fluorescence emission at 515 nm when it was excited at 439 nm. Upon the addition of various metal ions, the fluorescence intensity of HL showed a large fluorescence enhancement in the presence of Mg^{2+} and Zn^{2+} . Although Zn^{2+} also generated a certain fluorescence enhancement, it was far below the intensity caused by Mg^{2+} . In addition, other relevant metal ions such as Li^+ , Na^+ , K^+ , Ca^{2+} , Cu^{2+} , Co^{2+} , Mn^{2+} , Ni^{2+} , Ba^{2+} , Fe^{2+} , Cd^{2+} , Hg^{2+} , Pb^{2+} , Fe^{3+} , Cr^{3+} , and Al^{3+} had no significant effect on the fluorescence. The results suggested the

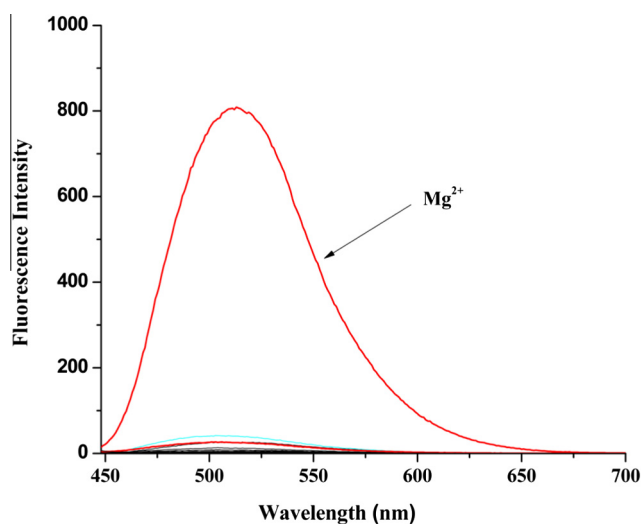


Fig. 3. Fluorescence spectra of HL (20 μM) upon the addition of metal salts (1.0 equiv.) of Li^+ , Na^+ , K^+ , Ag^+ , Al^{3+} , Ca^{2+} , Pb^{2+} , Cr^{3+} , Mn^{2+} , Fe^{2+} , Ni^{2+} , Co^{2+} , Fe^{3+} , Cu^{2+} , Ba^{2+} , Cd^{2+} , Hg^{2+} , Zn^{2+} and Mg^{2+} in acetonitrile ($\lambda_{\text{ex}} = 439 \text{ nm}$, slit widths: 3 nm/3 nm).

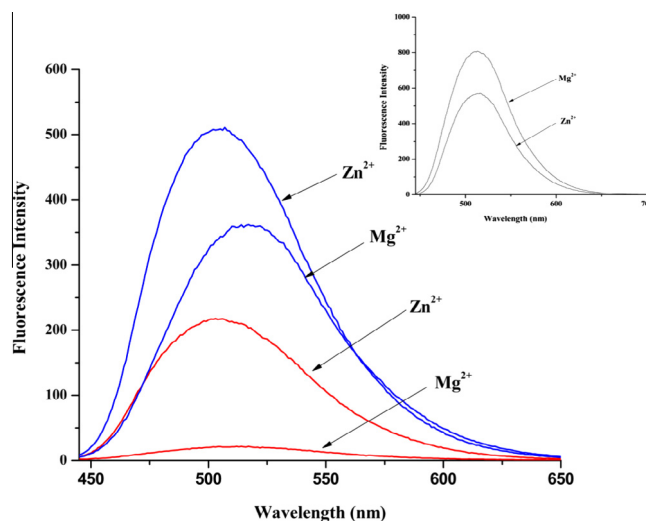


Fig. 4. The effect of ethanol–water in different ratio for the selectivity of HL (50 μM) for $\text{Mg}^{2+}/\text{Zn}^{2+}$ ($\lambda_{\text{ex}} = 439 \text{ nm}$, slit widths: 5 nm/3 nm). Blue line: in ethanol–water (v/v, 9:1). Red line: in ethanol–water (v/v, 4:1). Insert: The HL (10 μM) response to $\text{Mg}^{2+}/\text{Zn}^{2+}$ in absolute ethanol (slit widths: 3 nm/3 nm). (For interpretation of the references to color in this figure legend, the reader is referred to the web version of this article.)

sensor HL, having predominant recognition and selectivity, is of a good potential in the detection of Mg^{2+} .

To check the selectivity of HL for Zn^{2+} , the effect of ethanol–water in different ratio was studied as shown in Fig. 4. In absolute ethanol, the presence of Mg^{2+} and Zn^{2+} both resulted in fluorescence enhancement, and that the sensor seemed to have a better response to Mg^{2+} than Zn^{2+} . With the increase of the water content, the fluorescence intensity caused by Mg^{2+} and Zn^{2+} significantly decreased, more interesting, the fluorescence intensity of L-Mg was falling even faster. When the ratio of ethanol–water (v/v) was adjusted to 4:1, the fluorescence intensity of L-Mg was just negligible while the fluorescence intensity of L-Zn was low but detectable. Thus, the mixture of ethanol–water (v/v, 4:1) was

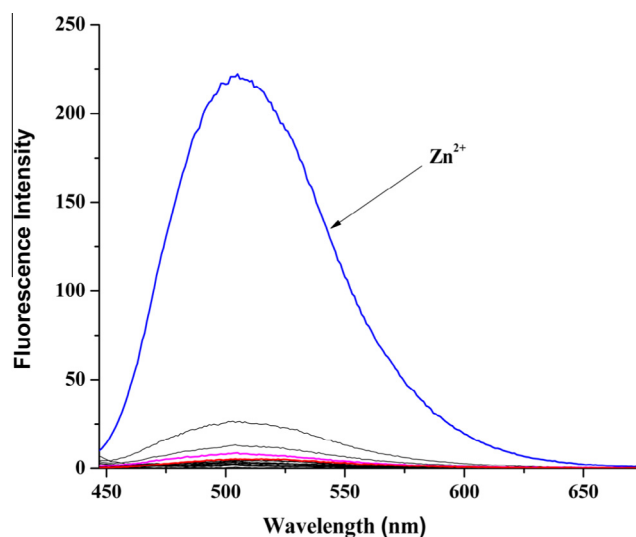


Fig. 5. Fluorescence spectra of HL (50 μM) upon the addition of metal salts (1.0 equiv.) of Li^+ , Na^+ , K^+ , Ag^+ , Al^{3+} , Ca^{2+} , Pb^{2+} , Cr^{3+} , Mn^{2+} , Fe^{2+} , Ni^{2+} , Co^{2+} , Fe^{3+} , Cu^{2+} , Ba^{2+} , Cd^{2+} , Hg^{2+} , Mg^{2+} and Zn^{2+} in ethanol–water (v/v, 4:1) ($\lambda_{\text{ex}} = 439 \text{ nm}$, slit widths: 5 nm/3 nm).

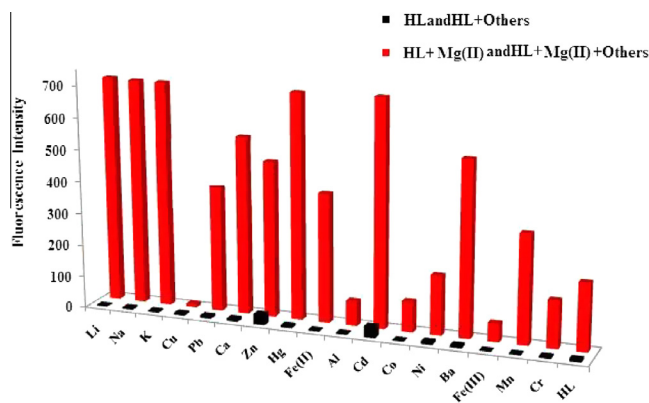


Fig. 6. Fluorescence intensity of HL and its complexation with Mg^{2+} in the presence of various metal ions in acetonitrile Black bar: HL (20.0 μM) and HL with 1.0 equiv. of Li^+ , Na^+ , K^+ , Ag^+ , Ca^{2+} , Hg^{2+} , Cr^{3+} , Mn^{2+} , Fe^{2+} , Ni^{2+} , Co^{2+} , Fe^{3+} , Cu^{2+} , Ba^{2+} , Cd^{2+} , Zn^{2+} and Al^{3+} stated. Red bar: 20.0 μM of HL and 1 equiv. of Mg^{2+} ; 20.0 μM of HL and 1.0 equiv. of Mg^{2+} with 1.0 equiv. of metal ions stated in acetonitrile ($\lambda_{ex} = 439$ nm, slit widths: 3 nm/3 nm). (For interpretation of the references to color in this figure legend, the reader is referred to the web version of this article.)

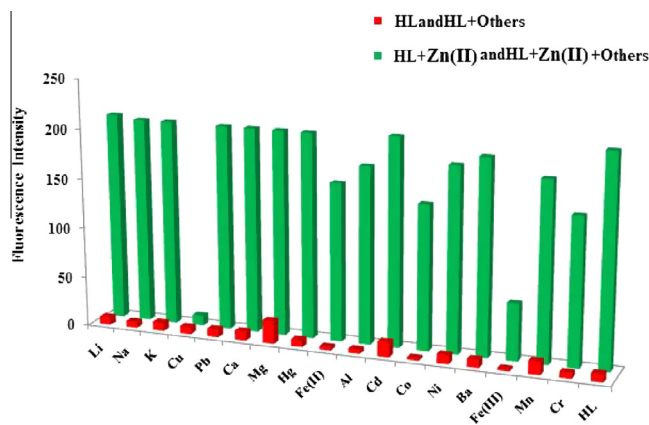


Fig. 7. Fluorescence intensity of HL and its complexation with Zn^{2+} in the presence of various metal ions in ethanol–water (v/v, 4:1). Red bar: HL (50.0 μM) and HL with 1.0 equiv. of Li^+ , Na^+ , K^+ , Ag^+ , Ca^{2+} , Hg^{2+} , Cr^{3+} , Mn^{2+} , Fe^{2+} , Ni^{2+} , Co^{2+} , Fe^{3+} , Cu^{2+} , Ba^{2+} , Cd^{2+} , Mg^{2+} and Al^{3+} stated. Green bar: 50.0 μM of HL and 1 equiv. of Zn^{2+} ; 50.0 μM of HL and 1.0 equiv. of Zn^{2+} with 1.0 equiv. of metal ions stated ($\lambda_{ex} = 439$ nm, slit widths: 5 nm/3 nm). (For interpretation of the references to color in this figure legend, the reader is referred to the web version of this article.)

selected as a test system. Moreover, as shown in Fig. 5, the sensor did not give any observable response for other relevant metal ions in ethanol–water (v/v, 4:1).

On the other hand, in the presence of Mg^{2+}/Zn^{2+} , the fluorescence spectrum displayed no emission peaks at 550 nm which was assigned to the characteristic emission of rhodamine. This phenomenon further confirmed the rhodamine core was in the ring closed isomeric form and the addition of Mg^{2+}/Zn^{2+} did not promote the ring-opened of the rhodamine spirolactam, the enhancement of the fluorescence intensity should be attributed to the interaction of the naphthalene moieties with Mg^{2+}/Zn^{2+} [35–36].

3.4. The practical applicability of HL

In order to evaluate the practical applicability of HL as a selective fluorescent sensor for Mg^{2+}/Zn^{2+} , two experiments should be conducted, one was competition experiment, the systems of other metal ions and Mg^{2+}/Zn^{2+} coexisted were examined in different

solvent, as shown in Figs. 6 and 7, we found that other competitive ions had no obvious interference with the detection of Mg^{2+}/Zn^{2+} except in the case of transition-metal ions, which be attributed to their inherent to the magnetic property. The other was the investigation of reversibility which also a prerequisite in developing fluorescent probe for the practical application. The reversibility of the recognition processes of HL was performed by adding Na_2EDTA (a bonding agent), as shown in Figs. 8 and 9, the addition of Na_2EDTA to a mixture of HL and Mg^{2+}/Zn^{2+} resulted in diminution of the fluorescence intensity, which indicated the regeneration of the free sensor HL, Upon the addition of Mg^{2+}/Zn^{2+} , the fluorescence intensity of HL showed significant fluorescence enhancement again.

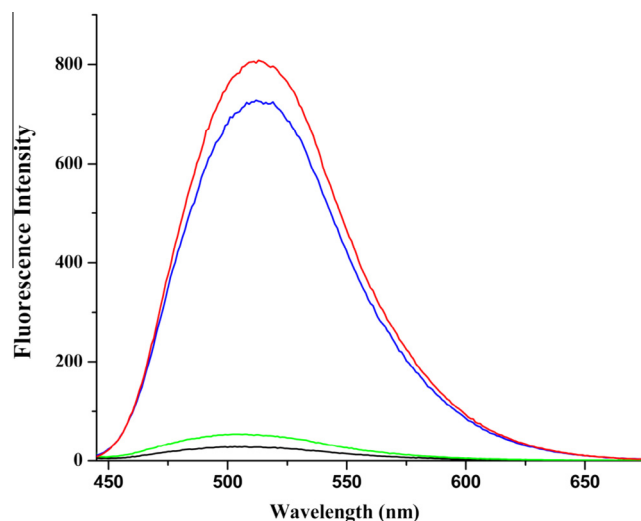


Fig. 8. The reversibility of recognition of Mg^{2+} was performed by adding Na_2EDTA in acetonitrile Black: HL, Red: HL+ Mg^{2+} , Green: HL+ Mg^{2+} + Na_2EDTA , Blue: HL+ Mg^{2+} + Na_2EDTA + Mg^{2+} , ($\lambda_{ex} = 439$ nm, slit widths: 3 nm/3 nm). (For interpretation of the references to color in this figure legend, the reader is referred to the web version of this article.)

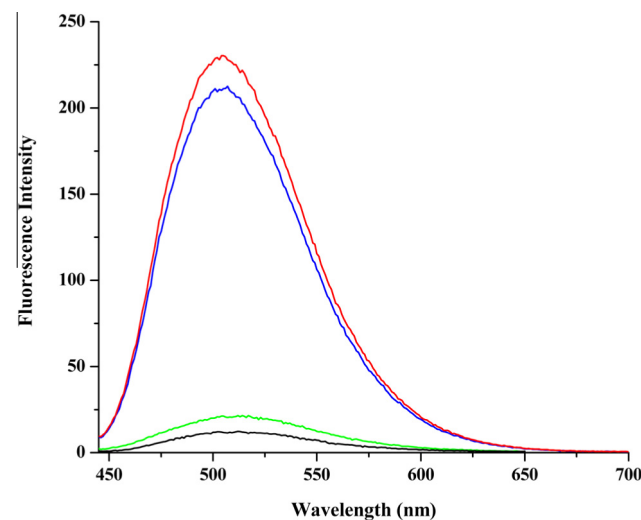


Fig. 9. The reversibility of recognition of Mg^{2+} was performed by adding Na_2EDTA in ethanol–water (v/v, 4:1). Black: HL, Red: HL+ Zn^{2+} , Green: HL+ Zn^{2+} + Na_2EDTA , Blue: HL+ Zn^{2+} + Na_2EDTA + Zn^{2+} , ($\lambda_{ex} = 439$ nm, slit widths: 5 nm/3 nm). (For interpretation of the references to color in this figure legend, the reader is referred to the web version of this article.)

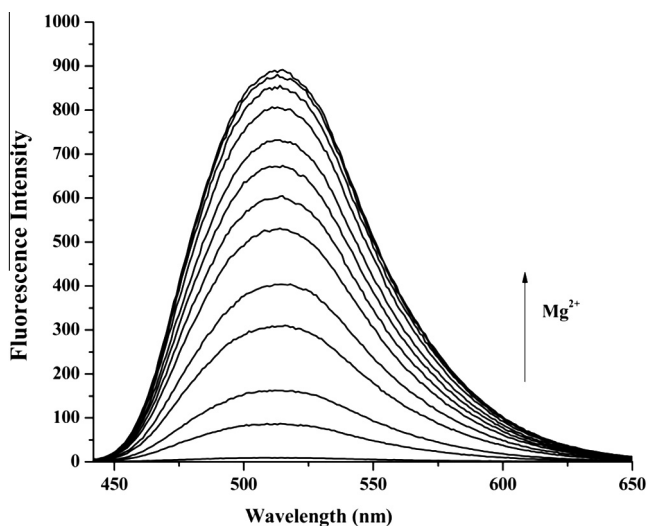


Fig. 10. Fluorescence spectra of HL (12.5 μM) in acetonitrile upon the addition of Mg^{2+} (0–1.2 equiv.) ($\lambda_{\text{ex}} = 439 \text{ nm}$, slit widths: 5 nm/3 nm).

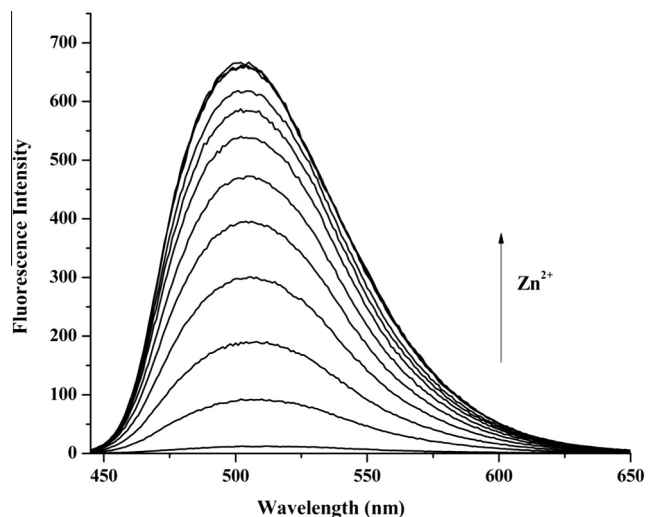


Fig. 11. Fluorescence spectra of HL (25 μM) in ethanol–water (v/v, 4:1) upon the addition of Zn^{2+} (0–1.2 equiv.) ($\lambda_{\text{ex}} = 439 \text{ nm}$, slit widths: 5 nm/5 nm).

Additionally, from the fluorescence titration profiles (Figs. 10 and 11), the detection limit of HL for $\text{Mg}^{2+}/\text{Zn}^{2+}$ was found to be $1.44 \times 10^{-6} \text{ M}/2.27 \times 10^{-6} \text{ M}$ (Figs. S6 and S7) which was

sufficiently low to enable the detection of micromolar concentrations of $\text{Mg}^{2+}/\text{Zn}^{2+}$ in many chemical and biological systems.

3.5. The complexation of HL with $\text{Mg}^{2+}/\text{Zn}^{2+}$

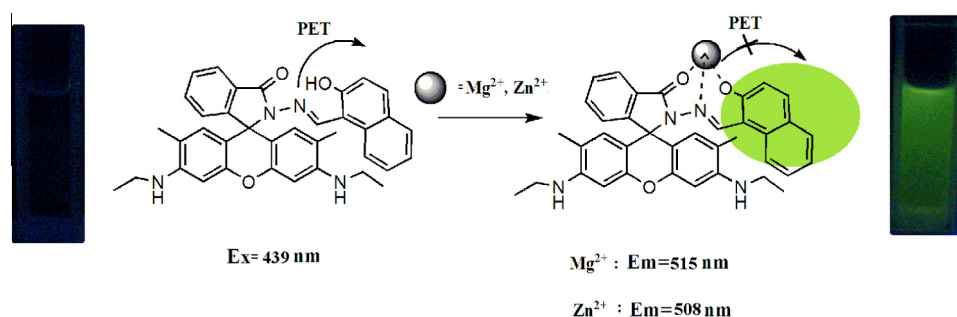
In order to understand the binding mode of HL and $\text{Mg}^{2+}/\text{Zn}^{2+}$, the sensor was treated with excessive $\text{Mg}^{2+}/\text{Zn}^{2+}$ ion, the fluorescence intensity reached the maximum in the presence of 1.0 equiv of $\text{Mg}^{2+}/\text{Zn}^{2+}$. Moreover, as shown in Figs. S8 and S9, when the molar fraction of $\text{Mg}^{2+}/\text{Zn}^{2+}$ was 0.5, the Job's plot of HL with $\text{Mg}^{2+}/\text{Zn}^{2+}$ exhibited a maximum fluorescence emission. The results all showed that HL and $\text{Mg}^{2+}/\text{Zn}^{2+}$ formed 1:1 ligand–metal complexes, which could be further conformed by the ESI-MS spectra in which the peak at m/z 646.98 was assignable to $[\text{HL}+\text{Mg}^{2+}+\text{CH}_3\text{CN}-1]^+$ (Fig. S10) and the peak at m/z 645.04 was assignable to $[\text{HL}+\text{Zn}^{2+}-1]^+$ (Fig. S11). Since the formation of 1:1 ligand–metal complexes was confirmed by Job's plot analysis and ESI/MS, in combination with the fluorescence titration, the binding constants of HL for $\text{Mg}^{2+}/\text{Zn}^{2+}$ have been estimated using the Benesi–Hildebrand equation, namely, The stability constants were determined as $1.16 \times 10^5/5.08 \times 10^4$ (Figs. S12 and S13).

3.6. The proposed mechanism

The above experiments suggested the rhodamine core always was in the ring closed isomeric form both in the presence of Mg^{2+} and Zn^{2+} and some reported fluorescent probes also shared some similarities to HL [37–43], the selective recognition of HL for $\text{Mg}^{2+}/\text{Zn}^{2+}$ should be attributed to the interaction of the naphthalene moieties with $\text{Zn}^{2+}/\text{Mg}^{2+}$ which inhibited photo-induced electron transfer (PET) process rather than the ring-opening of the rhodamine spirolactam. As shown in Scheme 2, it seemed that the lone pair electrons from the nitrogen atom of the $-\text{C}=\text{N}$ group to naphthalene moieties was responsible for the photoinduced electron-transfer (PET) process, which quenched fluorescence emission of the sensor. However, upon addition of $\text{Mg}^{2+}/\text{Zn}^{2+}$, the PET process was inhibited owing to the chelation of the nitrogen atom of the $-\text{C}=\text{N}$ group with $\text{Mg}^{2+}/\text{Zn}^{2+}$, as result, the quenched fluorescence could recur remarkably.

4. Conclusion

In summary, we have developed a rhodamine naphthalene-based chemosensor HL for Mg^{2+} and Zn^{2+} based on the inhibited photo-induced electron transfer (PET) process. The receptor showed “off–on” fluorescent responses toward Zn^{2+} in ethanol. When the solvent media was changed from ethanol to acetonitrile, the detection of the sensor could response to Mg^{2+} . In addition, the lower detection limit for $\text{Mg}^{2+}/\text{Zn}^{2+}$ was sufficiently low to enable



Scheme 2. Proposed mechanism for detection of $\text{Mg}^{2+}/\text{Zn}^{2+}$ by HL.

the detection of micromolar concentrations of Mg^{2+}/Zn^{2+} in many chemical and biological systems.

Acknowledgments

This work is supported by the National Natural Science Foundation of China (81171337), Gansu NSF (1308RJZA115).

Appendix A. Supplementary material

Supplementary data associated with this article can be found, in the online version, at <http://dx.doi.org/10.1016/j.ica.2015.06.017>.

References

- [1] M.J. Cromie, Y.X. Shi, T. Latifi, E.A. Groisman, *Cell* 125 (2006) 71.
- [2] G. Farruggia, S. Lotti, L. Prodi, M. Montalti, N. Zaccheroni, P.B. Savage, V. Trapani, P. Sale, F.I. Wolf, *J. Am. Chem. Soc.* 128 (2006) 344.
- [3] L. Jin, Z.J. Guo, Z.Y. Sun, A.L. Li, Q. Jin, M. Wei, *Sens. Actuators, B* 161 (2012) 714.
- [4] D. Ray, A. Nag, A. Jana, D. Goswami, P.K. Bharadwaj, *Inorg. Chim. Acta* 363 (2010) 2824.
- [5] S.B. Maity, P.K. Bharadwaj, *J. Lumin.* 155 (2014) 21.
- [6] J.D. Silva, R. Williams, *The Biological Chemistry of the Elements*, Oxford University Press, 2001.
- [7] W.H. Ding, W. Cao, X.J. Zheng, W.J. Ding, J.P. Qiao, L.P. Jin, *Dalton Trans.* 43 (2014) 6429.
- [8] T.M. Bray, W.J. Bettger, *Free Radical Biol. Med.* 8 (1990) 281.
- [9] L.J. Tang, M.J. Cai, P. Zhou, J. Zhao, K.L. Zhong, S.H. Hou, Y.J. Bian, *RSC Adv.* 3 (2013) 16802.
- [10] B.L. Vallee, K.H. Falchuk, *Physiol. Rev.* 73 (1993) 79.
- [11] R. McRae, P. Bagchi, S. Sumalekshmy, C.J. Fahrni, *Chem. Rev.* 109 (2009) 4780.
- [12] J. Li, Y. Zeng, Q. Hu, X. Yu, J. Guo, Z. Pan, *Dalton Trans.* 41 (2012) 3623.
- [13] Q. Hu, Y. Tan, M. Liu, J. Yu, Y. Cui, Y. Yang, *Dyes Pigm.* 107 (2014) 45.
- [14] Y. Ma, H. Chen, F. Wang, S. Kambam, Y. Wang, C. Mao, X. Chen, *Dyes Pigm.* 102 (2014) 301.
- [15] J.L. Smith, S. Xiong, W.R. Markesbery, M.A. Lovell, *Neuroscience* 140 (2006) 879.
- [16] A.I. Bush, W.H. Pettingell, M.D. Paradis, R.E. Tanzi, *J. Biol. Chem.* 269 (1994) 12152.
- [17] W. Gruber, J. Herbauts, *Analysis* 18 (1990) 12.
- [18] J. Quinero, C. Mongay, M.D. Guardia, *Microchem. J.* 43 (1991) 213.
- [19] Q.T. Cai, S.B. Khoo, *Anal. Chim. Acta* 276 (1993) 99.
- [20] X.D. Yu, P. Zhang, Q.R. Liu, Y.J. Li, X.L. Zhen, Y.M. Zhang, Z.C. Ma, *Mater. Sci. Eng., C* 39 (2014) 73.
- [21] S. Devaraj, Y.K. Tsui, C.Y. Chiang, Y.P. Yen, *Spectrochim. Acta, Part A* 96 (2012) 594.
- [22] P.S. Hariharan, N. Hari, S.P. Anthony, *Inorg. Chem. Commun.* 48 (2014) 1.
- [23] Y.Y. Ma, H. Liu, S.P. Liu, R. Yang, *Analyst* 137 (2012) 2313.
- [24] S.F. Zhao, N.Y. Chen, S.H. Mei, G.J. Sun, W.D. Hao, *Wuhan Li gong Da Xue Xue bao* 28 (2006) 73.
- [25] Y.T. Chen, S.Y. Mu, *J. Lumin.* 145 (2014) 760.
- [26] S. Pal, B. Sen, S. Lohar, M. Mukherjee, S. Banerjee, P. Chattopadhyay, *Dalton Trans.* (2015), <http://dx.doi.org/10.1039/c4dt03381g>.
- [27] H.A. Benesi, J.H. Hildebrand, *J. Am. Chem. Soc.* 71 (1949) 2703.
- [28] C.R. Lohani, J.M. Kim, S.Y. Chung, J. Yoon, K.H. Lee, *Analyst* 135 (2010) 2079.
- [29] T.J. Jia, W. Cao, X.J. Zheng, L.P. Jin, *Tetrahedron Lett.* 54 (2013) 3471.
- [30] D. Karak, S. Lohar, A. Sahana, S. Guha, A. Banerjee, D. Das, *Anal. Methods* 4 (2012) 1906.
- [31] V.P. Singh, K. Tiwari, M. Mishra, N. Srivastava, S. Saha, *Sens. Actuator, B-Chem.* 182 (2013) 546.
- [32] D. Karak, S. Lohar, A. Banerjee, A. Sahana, I. Hauli, S.K. Mukhopadhyay, J.S. Matalobos, D. Das, *RSC Adv.* 2 (2012) 12447.
- [33] M.H. Lee, T.V. Giap, S.H. Kim, Y.H. Lee, C. Kang, J.S. Kim, *Chem. Commun.* 46 (2010) 1407.
- [34] Y.X. Wu, J.B. Li, L.H. Liang, D.Q. Lu, J. Zhang, G.J. Mao, L.Y. Zhou, X.B. Zhang, W.H. Tan, G.L. Shen, R.Q. Yu, *Chem. Commun.* 50 (2014) 2040.
- [35] S. Lee, B.A. Rao, Y.A. Son, *Sens. Actuator, B-Chem.* 196 (2014) 388.
- [36] L.N. Wang, J.X. Yan, W.W. Qin, W.S. Liu, R. Wang, *Dyes Pigm.* 92 (2012) 1083.
- [37] X. Zhou, W. Yan, T. Zhao, Z.X. Tian, X. Wu, *Tetrahedron* 69 (2013) 9535.
- [38] J.M. An, Z.Y. Yang, M.H. Yan, T.R. Li, *J. Lumin.* 139 (2013) 79.
- [39] Y. Zhao, B.Z. Zheng, J. Du, D. Xiao, L. Yang, *Talanta* 85 (2011) 2194.
- [40] L. Cao, C.M. Jia, Y. Huang, Q. Zhang, N. Wang, Y.L. Xue, D.L. Du, *Tetrahedron Lett.* 55 (2014) 4062.
- [41] L. Fan, J.C. Qin, T.R. Li, B.D. Wang, Z.Y. Yang, *Sens. Actuator, B-Chem.* 203 (2014) 550.
- [42] S. Goswami, A. Manna, S. Paul, A.K. Maity, P. Saha, C.K. Quah, H.K. Fun, *RSC Adv.* 4 (2014) 34572.
- [43] V. Luxami, K. Paul Renukamal, S. Kumar, *RSC Adv.* 3 (2013) 9189.